

Lateral superlattices on parabolic quantum wells

S. Lindemann, M. Bänninger, T. Ihn, T. Heinzel,* S. E. Ulloa,† and K. Ensslin
Solid State Physics Laboratory, ETH Zürich, 8093 Zürich, Switzerland

K. Maranowski and A. C. Gossard

Materials Department, University of California, Santa Barbara, California 93106

(Received 29 August 2002; revised manuscript received 4 June 2002; published 29 October 2002)

Lateral superlattices have been fabricated on AlGaAs parabolic quantum wells. Two electrical subbands occupied in the growth direction lead to two sets of classical commensurability oscillations, each characterized by a different Fermi velocity. The dominant features can be explained by combining quantum-mechanical subband occupation and classical commensurability oscillations. The potential modulation of the lateral superlattice can be tuned by the nanopatterned top gate as well as by a back gate electrode.

DOI: 10.1103/PhysRevB.66.165317

PACS number(s): 73.50.-h, 72.20.-i, 72.90.+y

I. INTRODUCTION

Periodic lateral potentials imposed on two-dimensional electron gases (2DEG's) have lead to the observation of classical as well as quantum-mechanical phenomena. Commensurability or Weiss oscillations were observed in the magnetoresistance reflecting the commensurability of the lattice constant with the classical cyclotron diameter at the Fermi energy.¹⁻³ This effect appears in magnetoresistance experiments as a $1/B$ periodic oscillation, where B is the magnetic field applied perpendicular to the sample surface. This periodicity arises from the fact that the classical cyclotron diameter at the Fermi level

$$2R_c = 2 \frac{\hbar}{e} \frac{\sqrt{2\pi N_s}}{B} \quad (1)$$

is proportional to $1/B$. Here N_s is the two-dimensional carrier density. It was recognized early on that the effect can be explained in quasiclassical terms, namely, by a guiding-center-drift resonance in the periodically modulated two-dimensional electron gas.⁴ The only quantum-mechanical ingredient needed is the Fermi velocity of the electrons which is determined by the electron density.

Parabolic quantum wells represent unique model systems⁵ where several electrical subbands can be controllably occupied in the growth direction.⁶ In contrast to two-dimensional electron gases, where the electron occupancy in the second subband is usually a small fraction (typically less than 10%) of the total electron density,^{7,8} the electron densities in the two lowest subbands in parabolic quantum wells can be similar to within 30%.^{6,9} With carefully designed and fabricated back gate electrodes, one can control the electron density, the subband occupation, and the location of the electron distribution within the parabolic potential.¹⁰

In this paper we present experimental results obtained on a lateral superlattice fabricated on a parabolic quantum well. In contrast to previous experiments on 2DEG's several electronic subbands are occupied in this case. For two occupied subbands carriers with two different Fermi velocities coexist at the Fermi energy. We set out to explore the consequences of this situation for commensurability oscillations which are

predominantly a classical effect, as discussed above. We find that two sets of commensurability oscillations occur in the magnetoresistance, each related to a specific subband, despite the presence of intersubband scattering. Moreover, this structure has the added flexibility that the amplitude of the lateral potential modulation can be tuned by a patterned front gate electrode, and the homogeneous back gate used to tune the subband occupation. This control leads to a different ratio of the potential modulation and Fermi energy, which is the relevant parameter describing the magnetoresistance oscillations. A positive magnetoresistance at higher magnetic fields allows for a separate determination of the potential modulation amplitude. We find that there is a regime of gate voltages where strain dominates the modulation amplitude. In this situation, the transport data exhibit commensurability maxima which can be identified with the third harmonic of the potential modulation.

II. SAMPLES

The samples were grown by molecular-beam epitaxy using the $\text{Al}_x\text{Ga}_{1-x}\text{As}$ system. They contain a parabolic quantum well with x varying parabolically between 0 and 0.1 over a distance of 76 nm. The parabolic potential is placed between $x=0.3$ barriers with modulation doping on both sides to provide the carriers. An $n+$ doped GaAs, electrically separated by a layer of low-temperature grown GaAs,¹¹ is located $1.35\text{-}\mu\text{m}$ below the quantum well and serves as an efficient back gate electrode. The center of the parabolic potential is located 102-nm below the sample surface. For details of the sample structure see Ref. 10. At $T=4.2$ K and both gate voltages set to zero, the electron density is $N_s = 4.2 \times 10^{11} \text{ cm}^{-2}$ and the mobility $\mu = 210\,000 \text{ cm}^2/\text{Vs}$. The center of the parabola contains a 3-ML spike of $\text{Al}_{0.05}\text{Ga}_{0.95}\text{As}$ which can be used to monitor the position of the electron distribution in the well,¹⁰ but is otherwise not relevant for the present experiments.

The sample is patterned into a Hall geometry oriented along one of the cleavage directions of the crystal lattice. The voltage and current probes as well as the back gate are supplied with ohmic contacts. At low temperatures $T = 4.2$ K no detectable current ($I < 1$ pA) flows between back

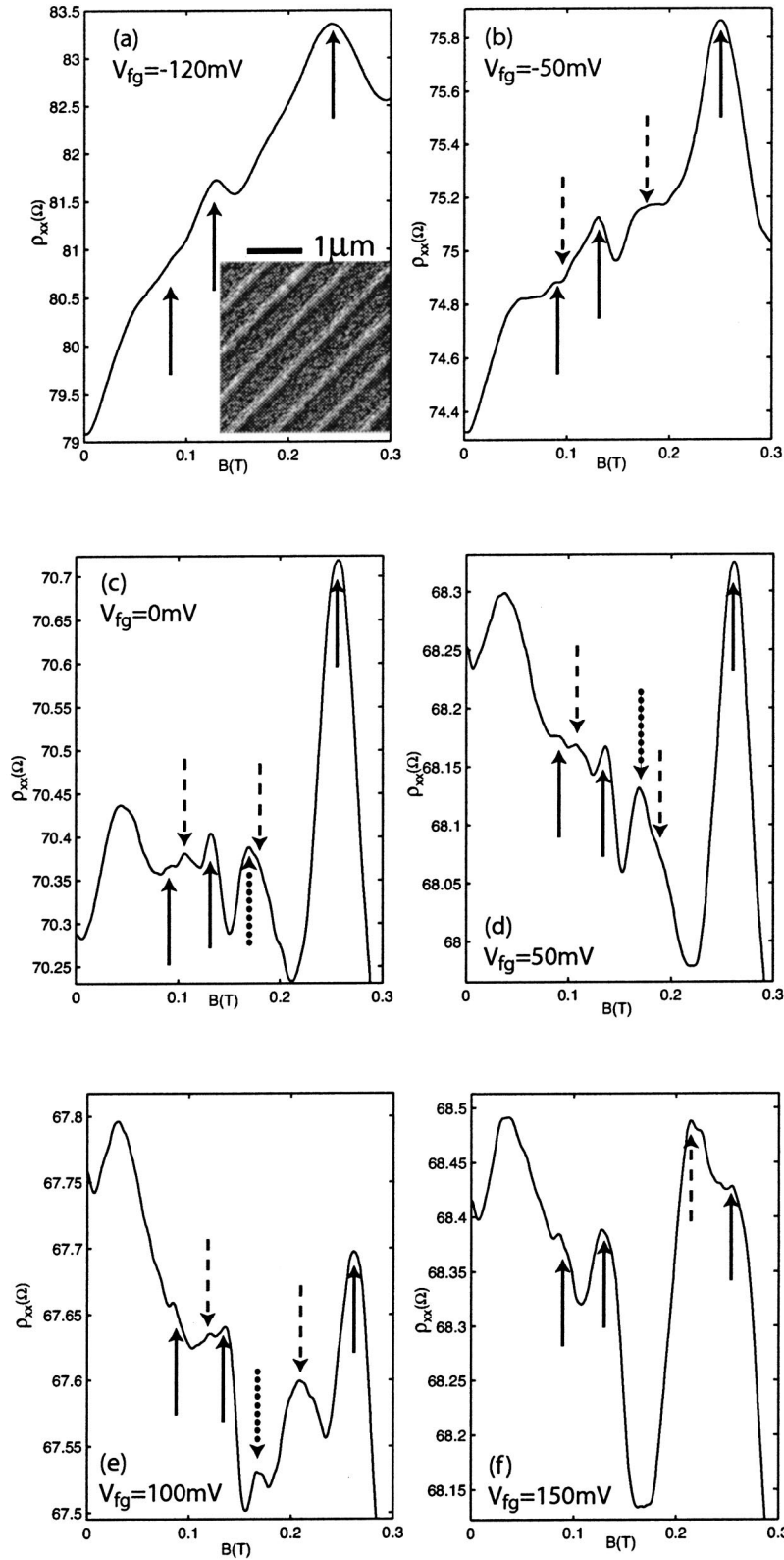


FIG. 1. (a) Magnetoresistance ρ_{xx} for fixed back gate voltage $V_{bg} = 0$ and several values of the front gate voltage. The arrows mark the positions of maxima calculated from Eq. (2) with the corresponding carrier densities as fitting parameters. Upper left panel (a) shows the case where only one subband is occupied. The inset in that panel shows an image of the nanostructured front gate electrode. (b)–(f) show the magnetoresistance in the regime where two subbands are occupied. The expected positions for the maxima of the commensurability oscillations for the lower (upper) subband are marked by solid (dashed) arrows. The features indicated by dotted arrows are discussed in the text.

gate and electron channel if $-3 \text{ V} < V_{bg} < +2 \text{ V}$. Using electron-beam lithography and a lift-off process a periodic one-dimensional array of gold wires (see inset in Fig. 1) with a period of 580 nm is patterned on the front (top) of the Hall bar. A lateral potential modulation is induced by appropriate

front gate voltages applied to the metal stripes.

The sample is measured in a temperature range $1.7 \text{ K} < T < 20 \text{ K}$ in the variable temperature insert of a ^4He cryostat. The resistance scale upon which the commensurability oscillations occur is relatively small, $\Delta R/R \approx 1\%$. For highly

resolved measurements, weak reproducible features occur superimposed on the commensurability oscillations, and are probably related to universal conductance fluctuations. In order to suppress these features we either measured at elevated temperatures ≈ 10 K or heated the electron gas by current levels as high as $5 \mu\text{A}$ which also helped to obtain a higher signal-to-noise ratio.

III. COMMENSURABILITY OSCILLATIONS

Figure 1 shows six magnetoresistance traces obtained for constant back gate voltage $V_{bg}=0$ and various front gate voltages V_{fg} . Starting from zero magnetic field, we first observe an increase in the magnetoresistance related to the drift of the guiding center along the equipotentials of the modulation. This is then overcome by magnetic breakdown at a critical field,¹² just before the well-known commensurability oscillations begin to occur.²⁻⁴ At yet higher magnetic field a positive parabolic magnetoresistance is observed (not shown), which can also be used to extract the magnitude of the potential modulation.¹³

The upper left curve (a) shows the regime where only the lowest subband is occupied and dominates the commensurability oscillations. The positions of the theoretically expected magnetoresistance maxima²⁻⁴ are given by

$$(n + \Phi)a = 2R_c, \quad (2)$$

where a is the lattice constant and n an integer indexing the commensurability condition. The arrows mark the positions of the maxima as calculated with the above equation (Refs. 2-4) with the carrier density as a fitting parameter and a fixed value of the phase factor Φ . The best fit to our experimental data occurs with a phase factor of $\Phi=0.18$ (instead of the theoretical value of $\frac{1}{4}$), in accordance with other experimental results.¹⁻³ Figures 1(b)-1(f) show experimental traces obtained for more positive top gate voltages where the second subband becomes occupied. The solid arrows mark maxima of the commensurability oscillations which can be ascribed to the lower subband, while the dashed arrows indicate maxima arising from the higher subband. The dotted arrows show additional features which will be discussed later. The positions of the solid and dashed arrows are obtained with a fixed phase factor of 0.18 and the carrier density, i.e., Fermi velocity, of the corresponding subband as a fitting parameter.

A Fourier analysis of the high-field SdH oscillations (not shown) reveals the carrier densities of the two subbands, N_s^0 and N_s^1 . If only the carrier density of the lower subband can be determined from this method (at low N_s^1 values) we have estimated the density in the higher subband from the Hall density minus the density in the lower subband.

The carrier densities are also determined from the previously described fit of the positions of the commensurability maxima. These two ways of extracting densities are presented in Fig. 2. There is reasonable agreement considering the rather different measurements, and the fact that the commensurability maxima are superimposed on a strong background. We conclude at this point that the system can be

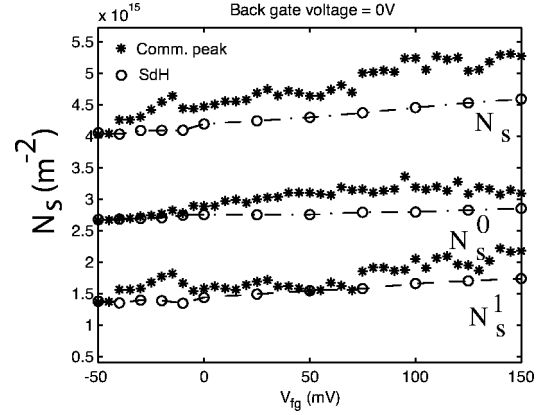


FIG. 2. Carrier density in the lower and N_s^0 , and upper subband, N_s^1 , as well as the total carrier density $N_s = N_s^0 + N_s^1$ extracted either from SdH and Hall measurements (circles) or from the fitting of the commensurability oscillations (asterisks) as presented in Fig. 1. The dashed lines are guides to the eye.

basically described by existing theories for commensurability oscillations if one ascribes two different Fermi velocities to the electrons residing in the two subbands, and ignores their possible mixing due to the small fields in the growth direction produced by the modulation, and the intersubband scattering present.

The carrier mobility in the second subband can be rather low for low occupancies.⁶ It is surprising that while SdH oscillations arising from the second subband are hardly discernible, the corresponding commensurability oscillations are well developed. The explanation of this observation is that for SdH oscillations, the small-angle quantum scattering time is the most relevant. For commensurability oscillations, however, it has been shown that a modified Drude scattering time which depends explicitly on electron density has to be considered,¹⁴ in order to get quantitative agreement between theory and experiment in the one-subband case. Here we have, in principle, the additional parameter of the intersubband scattering time. A detailed understanding of the microscopic scattering events as they influence the experimental line shape is required in order to further clarify their different roles, without a profusion of free parameters.

For an intermediate range of gate voltages we observe a different set of maxima in the magnetoresistance which cannot be explained by the commensurability oscillations of neither the lower subband nor of the upper subband. If we consider a strong third harmonic of the potential modulation³ and use the Fermi velocity of the electrons in the lower subband we obtain the maxima positions as indicated by the dotted arrows. We will come back to this point after the discussion of the potential modulation amplitude.

IV. AMPLITUDE OF POTENTIAL MODULATION

In our samples we can tune the carrier density as well as the amplitude of the potential modulation V_0 by the homogeneous back gate, as well as by the nanostructured top gate. We can therefore realize situations where the carrier densities in the respective subbands are kept constant and the potential

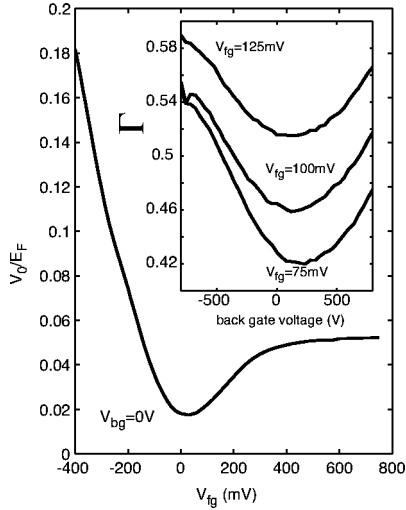


FIG. 3. Potential modulation versus front gate voltage for constant $V_{bg}=0$. The inset shows the Γ prefactor of the B -parabolic fit as a function of back gate voltage for various values of the top gate voltage.

modulation is varied. The modulation amplitude can be extracted from the positive magnetoresistance after the last maximum of the magnetoresistance oscillations¹³ following a B^2 dependence

$$\frac{\Delta\rho_{xx}}{\rho_{xx}} = (\omega_c\tau)^2 \left(\frac{V_0}{E_F}\right)^2. \quad (3)$$

Here ω_c is the cyclotron frequency $\omega_c = eB/m$, τ is the scattering time, V_0 is the amplitude of the potential modulation, E_F is the Fermi energy, and the high-field condition $a \gg R_c$ has been used.¹³ Another possibility is to analyze the positive magnetoresistance peak at very low magnetic fields describing the onset of magnetic breakdown.¹² The results obtained by these procedures differ by less than 50%, and the qualitative behavior as a function of the two gate voltages is the same. In the following we present only results obtained using the positive magnetoresistance in the high magnetic-field regime after the commensurability oscillations (following Geim *et al.*¹³) since this method can be used for a meaningful analysis over a wider gate voltage range.

We notice that a positive magnetoresistance can also arise if two subbands with rather different carrier mobilities are occupied with different densities.¹⁵ This effect occurs at low magnetic fields and is weak in the present case, since the carrier densities in the two subbands here are of the same order of magnitude.

The evaluation of the potential amplitude V_0 requires the Fermi energy of the electrons, as per Eq. (3). Since the electrons in the lower subband are responsible for the dominant features in the magnetoresistance (commensurability as well as SdH oscillations) we take the Fermi velocity v_F^0 of the electrons in the lower subband. A value of the Fermi velocity based on the total electron density, on the other hand, would change our results by at most a factor of $\sqrt{2}$, and the qualitative interpretation of the data is not affected.

Figure 3 shows the potential modulation as a function of

top gate voltage for constant $V_{bg}=0$, i.e., the same parameters as used for the curves in Figs. 1 and 2. The potential modulation starts from a rather large value at negative top gate voltages, goes through a minimum around $V_{fg} \approx 0$, and then increases again. It never reaches zero, as expected for a purely electrostatic potential modulation induced by the gate potential. This indicates that for gate voltages close to the minimum, the strain-induced potential modulation due to the mere presence of the gate stripes dominates the potential modulation.¹⁶ At higher and lower gate voltages the potential modulation can be tuned by the electric field (although this saturates at high V_{fg} values due to the charging of deep centers in the top barrier material). The pronounced dependence of the potential modulation on top gate voltage applied to the gate stripes is expected, since the top gate voltage can change the electron density as well as the potential modulation.

A potential modulation which is purely induced by the modulated gate potential leads predominantly to a sinusoidal potential shape. If the potential modulation, however, is dominated by strain then higher harmonics become relatively stronger. Additional features, as indicated by the dotted arrows in Fig. 1, start to appear once the potential modulation is close to its minimum in Fig. 3. This supports our interpretation of the additional structures in the magnetoresistance in terms of consequences of a reasonably strong third harmonic of the potential modulation as indicated in Fig. 1. There are ranges in magnetic field where the features related to the third harmonic of the lower subband and the first harmonic of the upper subband are not easy to distinguish.

The back gate voltage is expected to modulate the relative potential modulation V_0/E_F only by the modified Fermi energy of the electron gas as a function of density, since the screening length does not depend on the carrier density in a two-dimensional system. In the range of back gate voltages investigated (see inset of Fig. 3) the density changes by 20%, in the range $4 - 5 \times 10^{11} \text{ cm}^{-2}$. We therefore expect a similar 20% change in the value of V_0/E_F . In this regime, where the third subband starts to become weakly populated,⁶ the total mobility of the system undergoes a strong nonmonotonic behavior. We should notice that the scattering time of the lower subband displays a weak maximum and at a different total carrier density than the maximum of the total mobility.¹⁵ Since these effects are typically larger than 20%, it is difficult to extract the precise back gate dependence of the relative potential modulation. A model based on the contribution of two subbands to the conductivity in fact illustrates this difficulty. Using such an approach, after appropriate matrix inversion, leads to the following expression for the magnetoresistance change at high field, $R_c/a \ll 1$,

$$\frac{\Delta\rho_{xx}}{\rho_{xx}} \simeq \Gamma B^2, \quad (4)$$

with the parameter Γ

$$\Gamma = \frac{e^2}{m^{*2}} \frac{\sum_i \tau_i \left(v_F^i \frac{V_0}{E_F^i} \right)^2}{\sum_i v_F^{i2} / \tau_i}. \quad (5)$$

Here τ_i is the scattering time of subband i , and E_F^i and v_F^i the Fermi energy and velocity of subband i . The Fermi energies of the two subbands differ by less than 30%, i.e., $E_F^0 \simeq E_F^1 \simeq E_F$. In this limit, the equation above reduces to

$$\Gamma \simeq \frac{e^2}{m^{*2}} \tau_0 \tau_1 \left(\frac{V_0}{E_F} \right)^2. \quad (6)$$

In this expression, the scattering times τ_0 and τ_1 are nearly monotonic functions of the back gate potential, increasing with increasing voltage. The Fermi energy, on the other hand, decreases monotonically with voltage, resulting in a rather weak dependence of the Γ factor in the parabolic fit with back gate voltage. In contrast, the inset in Fig. 3 shows this prefactor Γ versus back gate voltage, for various values of the top gate voltage. There is a clear minimum in this parameter as a function of back gate voltage. The position of this minimum shifts approximately with the maximum observed in the total mobility versus back gate voltage once the third subband becomes populated.⁶ It is therefore evident that a more detailed analysis would require a better understanding of how the carriers in different subbands with different densities and mobilities give rise to the parabolic magnetoresistance fitted here. It is interesting to notice that extracting values of V_0/E_F using Eq. (3) and the value of Γ

in the inset would yield values of a few percent, comparable to the values near the minimum in Fig. 3. Moreover, the typical range of tunability of the potential modulation is close to the estimated value of 20% described before.

V. CONCLUSION

We have demonstrated that classical commensurability oscillations induced by a lateral superlattice can be modified by the occupation of a second quantum-mechanical subband. This fascinating interplay between quantum-mechanical and classical properties can be used to learn more about parabolic quantum wells. Most experimentally observed features can be accounted for by treating the two subbands as two independent carrier systems. We find also additional maxima in the low-field magnetoresistance which are related to the third harmonic of the potential modulation. These features are found for specific gate voltages where the strain-induced potential modulation dominates. Our systems, equipped with homogeneous back and patterned top gate electrodes, allowed us to separate the effects of screening and electrostatically induced modulation on the effective amplitude of the potential modulation in the electron gas. We expect that parabolic quantum wells which represent ideal model systems at the crossover from two to three dimensions continue to contribute to our understanding of quantum effects in semiconductor nanostructures.

ACKNOWLEDGMENT

We are grateful to the Swiss Science Foundation (Schweizerischer Nationalfonds) for financial support.

*Present address: Fakultät für Physik, Universität Freiburg i.Br., 79104 Freiburg, Germany.

†Present address: Department of Physics and Astronomy, Ohio University, Athens, OH 45701-2979

¹D. Weiss, K. v. Klitzing, K. Ploog, and G. Weinmann, *Europhys. Lett.* **8**, 179 (1989).

²R. R. Gerhardts, D. Weiss, and K. v. Klitzing, *Phys. Rev. Lett.* **62**, 1173 (1989).

³R. W. Winkler, J. P. Kotthaus, and K. Ploog, *Phys. Rev. Lett.* **62**, 1177 (1989).

⁴C. W. J. Beenakker, *Phys. Rev. Lett.* **62**, 2020 (1989).

⁵A. C. Gossard, *IEEE J. Quantum Electron.* **22**, 1649 (1986).

⁶K. Ensslin, A. Wixforth, M. Sundaram, P. F. Hopkins, J. H. English, and A. C. Gossard, *Phys. Rev. B* **47**, 1366 (1993).

⁷H. L. Stoermer, A. C. Gossard, and W. Wiegmann, *Solid State Commun.* **41**, 707 (1982).

⁸K. Ensslin, D. Heitmann, and K. Ploog, *Phys. Rev. B* **37**, 10 150 (1988).

⁹K. Ensslin, C. Pistitsch, A. Wixforth, M. Sundaram, P. F. Hopkins, and A. C. Gossard, *Phys. Rev. B* **45**, 11 407 (1992).

¹⁰G. Salis, B. Graf, K. Ensslin, K. Campman, K. Maranowski, and A. C. Gossard, *Phys. Rev. Lett.* **79**, 5106 (1997).

¹¹K. D. Maranowski, J. P. Ibbetson, K. L. Campman, and A. C. Gossard, *Appl. Phys. Lett.* **66**, 3459 (1995).

¹²P. H. Beton, M. W. Dellow, P. C. Main, E. S. Alves, L. Eaves, S. P. Beaumont, and C. D. W. Wilkinson, *Phys. Rev. B* **43**, 9980 (1991).

¹³A. K. Geim, R. Taboryski, A. Kristensen, S. V. Dubonos, and P. E. Lindelof, *Phys. Rev. B* **46**, 4324 (1992).

¹⁴P. Bøggild, A. Boisen, K. Birkelund, C. B. Sørensen, R. Taboryski, and P. E. Lindelof, *Phys. Rev. B* **51**, 7333 (1995).

¹⁵G. Salis, P. Wirth, T. Heinzel, T. Ihn, K. Ensslin, K. Maranowski, and A. C. Gossard, *Phys. Rev. B* **59**, R5304 (1999).

¹⁶I. A. Larkin, J. H. Davies, A. R. Long, and R. Cusc, *Phys. Rev. B* **56**, 15 242 (1997).